Substitutions in the *N*-Glycan Core as Regulators of Biorecognition: The Case of Core-Fucose and Bisecting GlcNAc Moieties†

Sabine André,*,‡ Tibor Kožár,§ Ralf Schuberth,|| Carlo Unverzagt,|| Shuji Kojima,⊥ and Hans-Joachim Gabius‡

Institute of Physiological Chemistry, Faculty of Veterinary Medicine, Ludwig-Maximilians-University Munich, Veterinärstrasse 13, D-80539 Munich, Germany, Institute of Experimental Physics, Department of Biophysics, Slovak Academy of Sciences, Watsonova 47, SK-01001 Kosice, Slovak Republic, Bioorganic Chemistry, Building NW1, University of Bayreuth, D-95440 Bayreuth, Germany, and Faculty of Pharmaceutical Sciences, Tokyo University of Science, Yamazaki 2641, Noda-City, Chiba 278-8510, Japan

Received January 10, 2007; Revised Manuscript Received March 6, 2007

ABSTRACT: Core fucosylation and the bisecting *N*-acetylglucosamine residue are prominent natural substitutions of the *N*-glycan core. To address the issue of whether these two substituents can modulate ligand properties of complex-type biantennary *N*-glycans, we performed chemoenzymatic synthesis of the respective galactosylated and α2,3/6-sialylated *N*-glycans. Neoglycoproteins were then produced to determine these glycans' reactivities with sugar receptors in solid-phase assays and with tumor cells in vitro as well as their in vivo biodistribution profiles in mice. Slight protein-type-dependent changes were noted in lectin binding, including adhesion/growth-regulatory galectins as study objects, when the data were related to properties of *N*-glycans without or with only one core substituent. Monitoring binding in vitro revealed cell-type-dependent changes. They delimited the ligand activity of this glycan type from that of chains with un- and monosubstituted cores. A markedly prolonged serum half-life was conferred to the neoglycoprotein by the galactose-terminated *N*-glycan, which together with increased organ retention of all three neoglycoproteins underscores the conspicuous relevance for glycoengineering of pharmaproteins. The predominant presentation of the two branches in the disubstituted *N*-glycan as extended (α1,3-antenna) and backfolded (α1,6-antenna) forms, revealed by molecular dynamics simulations, can underlie the measured characteristics. These results obtained by a combined strategy further support the concept of viewing *N*-glycan core substitutions as non-random additions which exert a modulatory role on ligand properties. Moreover, our data inspire us to devise new, non-natural modifications to realize the full potential of glycoengineering for diagnostic and therapeutic purposes.

Glycosylation is known to alter a series of protein parameters such as solubility, charge, resistance to proteases, and immunogenicity (*1*, *2*). Beyond these rather general effects, the non-random nature of the biosynthesis of sugar chains in glycoproteins implies they have more specific functions such as a role as a signal in biorecognition (*3*, *4*). As a consequence, deficiencies are expected to arise in vitro and in vivo after distinct aspects of glycan production are impaired. Fittingly, the analysis of several deletion mutants for glycosyltransferases initiating synthesis of complex-type *N*-glycans or distinct branches thereof bears out the fundamental merit of this assumption (*5*). Even rather subtle modifications are apparently not negligible. This is illustrated by the influence of core fucosylation on binding of epidermal growth factor to its receptor and ensuing signal routing as well as the inhibitory effect of the presence of this fucose moiety on deglycosylation by murine *N*-glycanase (*6*, *7*). When relevant for docking of lectins, e.g., adhesion/growth-regulatory endogenous galectins (*8*), structural diversity dependent on *N*-glycan branching has been attributed to a decreasing level of constitutive endocytosis of the epidermal growth factor receptor or glucose transporter 2 (*9*, *10*). Moreover, cell-type-specific branch-end glycosylation governing carbohydrate-mediated contacts between leukocytes and endothelial cells or neutrophils and dendritic cells (*11*) and ensuing signal transduction (*12*) signifies the far-reaching potential of glycans as molecular signals. Altogether, these results and implications prompt close examination of structure−activity profiles of natural glycans.

Toward this end, we have set up activity assays (a) with a panel of lectins, including galectins mentioned above, (b) with tumor cells in vitro, and (c) with mice in vivo and standardized their application with neoglycoproteins carrying the complex-type biantennary *N*-glycan nonasaccharide (*13*). Taking advantage of the progress in chemoenzymatic synthesis, we have successively been able to prepare its major natural variants. Thus, the so far unresolved issue of defining structure−(ligand) activity profiles of *N*-glycans can now be addressed systematically. A pertinent question concerns the

† This work was supported by the Deutsche Forschungsgemeinschaft, an EC Marie Curie Research Training Network (Contract MRTN-CT-2005-019561), the Mizutani Foundation for Glycoscience (Tokyo, Japan), and the Verein zur Förderung des biologisch-technologischen Fortschritts in der Medizin e. V. (Heidelberg, Germany).

* To whom correspondence should be addressed. Telephone: +49-(0)89-2180 3279. Fax: +49-(0)89-2180 2508. E-mail: Sabine.Andre@lmu.de.

‡ Ludwig-Maximilians-University Munich.

§ Slovak Academy of Sciences.

|| University of Bayreuth.

⊥ Tokyo University of Science.

10.1021/bi7000467 CCC: $37.00
Published on Web 05/12/2007

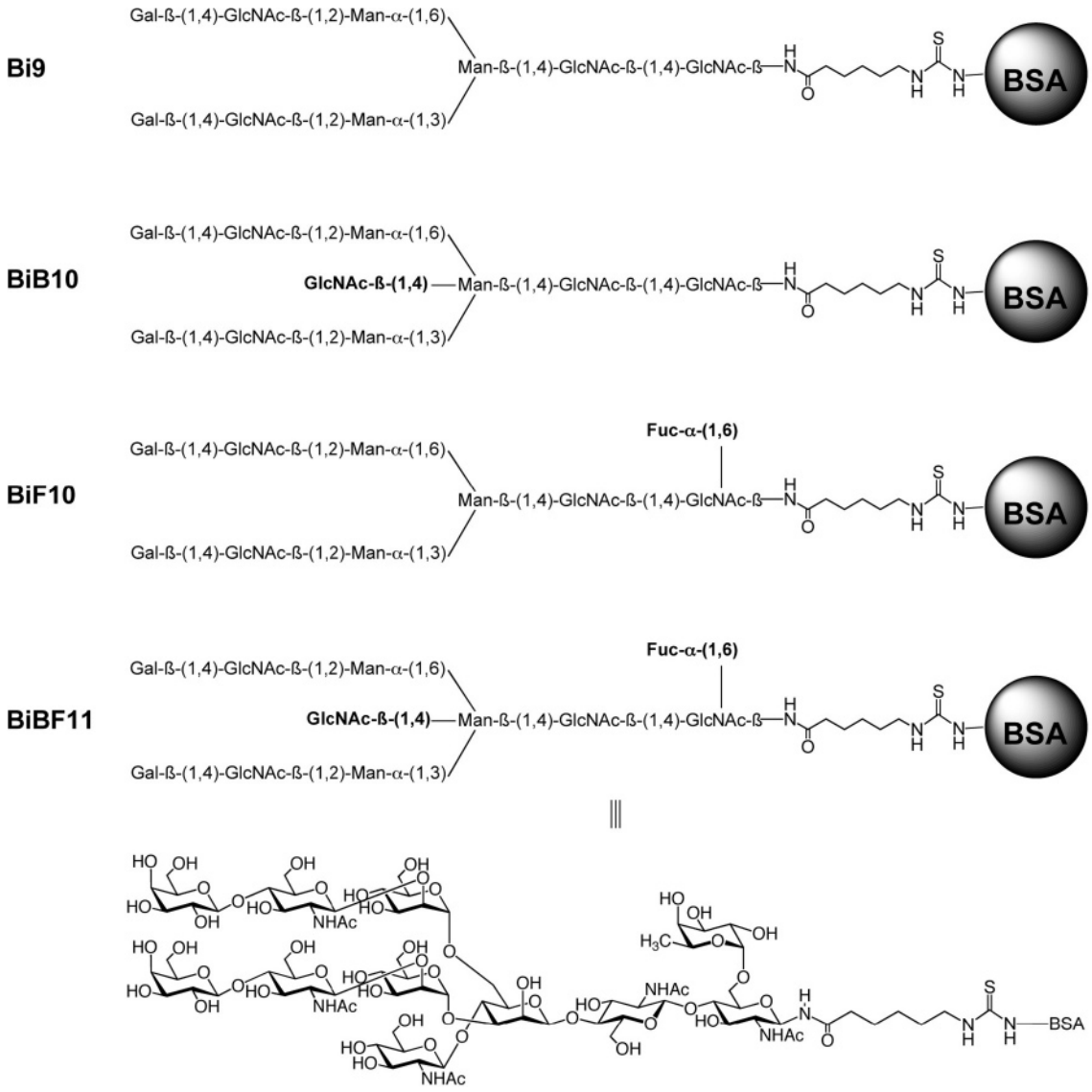

FIGURE 1: Structures of the complex-type biantennary nonasaccharide without core substitution (Bi9), the two monosubstituted decasaccharides with either the bisecting GlcNAc (B) (BiB10) or the core-fucose unit (F) (BiF10), and the disubstituted undecasaccharide BiBF11, which is drawn in two modes.

presence of core substitutions, i.e., the incorporation of a bisecting *N*-acetylglucosamine (GlcNAc)[1] moiety and core fucosylation (Figure 1). We herein focus on the compound bearing both substitutions mentioned above, which turn the biantennary nonasaccharide (Bi9) into the undecasaccharide BiBF11 (Figure 1).

This disubstituted *N*-glycan is, among others, abundant on human HuH-6 hepatoblastoma cells (*14*) and an integral part of human immunoglobulin G (IgG) at Asn297 in both C_H2 domains of the heavy chains' F_c region (*15*, *16*). At this site, a strong modulatory role of the *N*-glycan's fucose residue on binding of IgG to $F_c\gamma$ receptors by protein−protein interaction and as a consequence antibody-dependent cellular cytotoxicity was noted (*17*−*19*). The presence of the BiBF11 epitope on LEC10 Chinese hamster ovary (CHO) mutant cells was associated with the reduced toxicity of ricin, indicating a decreased ligand activity (*20*−*22*). Because this type of disubstitution, but also concomitant alteration of the extent of branching and branch-end galactosylation, can factor into a reduced capacity of the mutant cells to bind lectin (*22*), the issue of whether the introduction of both sugar units into the core of complex-type biantennary *N*-glycans may modulate lectin affinity in this special case, but also in a more general context, is not resolved. This is why we addressed the following fundamental question using a combined strategy, pairing preparative carbohydrate chemistry with biochemical/cell biological activity assays: Will lectin affinity, cell binding, and clearance from serum be affected by presence of these substitutions?

MATERIALS AND METHODS

Synthetic and Analytical Procedures. NMR spectra were recorded on a Bruker AMX 500 spectrometer. HPLC separations were performed on a model 2249 Pharmacia (Freiburg, Germany) LKB gradient system equipped with a model VWM 2141 Pharmacia LKB Detector. For size exclusion chromatography, a Pharmacia Hi Load Superdex 30 column (600 mm × 16 mm) was used. RP-HPLC was

[1] Abbreviations: ASF, asialofetuin; BSA, bovine serum albumin; CHO, Chinese hamster ovary; GlcNAc, *N*-acetylglucosamine; IgG, immunoglobulin G; MD, molecular dynamics; SAP, serum amyloid P component; VAA, *Viscum album* agglutinin.

performed on a Macherey-Nagel (Düren, Germany) Nucleogel RP 100-10 column (300 mm × 25 mm). Carbohydrate-free bovine serum albumin (BSA) and bovine β-1,4-galactosyltransferase were purchased from Sigma (Munich, Germany), and alkaline phosphatase (calf intestine, molecular biology grade) was from Roche Diagnostics (Heidelberg, Germany). UDP-Galactose was a generous gift from Roche Diagnostics. ESI-TOF mass spectra were recorded using a methanol/water mixture as a solvent on a Micromass LCT spectrometer connected to an Agilent HP 1100 HPLC apparatus, and MALDI-TOF mass spectra were recorded on a Bruker Reflex III instrument using the linear mode and an acceleration voltage of 20 kV. For sample preparation in MALDI-TOF mass spectrometry, a solution of a neoglycoprotein (1 μL, 7 mg/mL) in 0.1% TFA was mixed with 1.5 μL of 33% acetonitrile in 0.1% TFA and 2.5 μL of a saturated solution of sinapinic acid in 0.1% TFA, the mixture thereafter being dried under high vacuum. The structures of synthetic *N*-glycans, whose chemical preparation up to the stage of the nonasaccharide with an aminohexanoyl spacer was reported previously (*23*), were confirmed by the following two-dimensional NMR experiments: TOCSY, NOESY, HMQC, HMQC-COSY, HMQC-DEPT, and HMQC-TOCSY. As graphically outlined in Figure 2, the prerequisite for conjugation of the derivatized *N*-glycans to the carrier protein was met by conversion of the amino group of the spacer in compound **2**, **3**, or **4** into the corresponding isothiocyanate, as described previously (*13*). In essence, 6-aminohexanoyl-*N*-glycan (0.195 μmol = 0.41 mg of **2** or 0.52 mg of **3** or **4**) was dissolved in sodium hydrogen carbonate (100 μL, 10 mg/mL) in a 1.5 mL plastic vial followed by addition of dichloromethane (100 μL) and thiophosgene (0.5 μL, 1.97 μmol). The biphasic mixture was stirred vigorously. After 2 h (TLC, 2:1 2-propanol/1 M ammonium acetate mixture), the mixture was centrifuged, and the aqueous phase was separated. Subsequently, the organic phase was extracted twice with solutions of sodium hydrogen carbonate (50 μL, 10 mg/mL). The combined aqueous phases were next extracted twice with dichloromethane (250 μL). BSA (1.15 mg in 8 mL of water) was added to the aqueous solution of each isothiocyanate derivative, and the reaction vials were kept for 6 days at ambient temperature. Thereafter, the reaction mixture was centrifuged, and the clear supernatant was fractionated by gel filtration [Pharmacia Hi Load Superdex 30 (600 mm × 16 mm); eluent, 0.1 M ammonium hydrogen carbonate; flow rate, 0.75 mL/min; detection at 214 and 254 nm] in each case and then lyophilized. Yields were as follows: 1.05 mg of BiBF11, 0.94 mg of BiBF1323, and 0.96 mg of BiBF1326; R_f amine **2** = 0.17 (2:1 2-propanol/1 M ammonium acetate mixture), R_f isothiocyanate = 0.85 (1.5:1 2-propanol/1 M ammonium acetate mixture); R_f amine **3** = 0.14 (2:1 2-propanol/1 M ammonium acetate mixture), R_f isothiocyanate = 0.73 (2:1 2-propanol/1 M ammonium acetate mixture); R_f amine **4** = 0.12 (2:1 2-propanol/1 M ammonium acetate mixture), R_f isothiocyanate = 0.68 (2:1 2-propanol/1 M ammonium acetate mixture). Quality controls of the neoglycoproteins and determination of the extent of glycan conjugation were performed by gel electrophoretic analysis and MALDI-TOF mass spectrometry. The resulting products were then either directly used in the solid-phase assays, labeled with the *N*-hydroxysuccinimide ester derivative of biotin under standard conditions, or radioiodinated (*13*). For convenient comparison of these common substituted *N*-glycans in terms of terminology, we followed the previously applied system of compound definition to refer to the complex-type biantennary nonasaccharide as Bi9 (*13*), with the two substitutions (bisecting GlcNAc = B, core-fucose unit = F) then resulting in BiBF11 and its two α2,3/α2,6-sialylated tridecasaccharides BiBF1323 and BiBF1326 (*24*, *25*), as presented in Figure 1 and Figure 2.

Biorecognition Studies. The standard protocols for testing *N*-glycan-containing neoglycoproteins in solid-phase, cell binding, and biodistribution assays were followed without changes to allow valid comparison with previous studies (*13*, *24*, *25*). Human galectins, the β-galactoside-binding IgG fraction from human serum, and the galactoside-binding toxin/agglutinin from mistletoe [*Viscum album* agglutinin (VAA)] were purified after recombinant production or from serum or plant extract by affinity chromatography on lactosylated Sepharose 4B as a crucial step, then subjected to analytical quality controls by one- and two-dimensional gel electrophoresis, mass spectrometry, ultracentrifugation, and gel filtration, and labeled via biotinylation under activity-preserving conditions with determination of the extent of marker incorporation by two-dimensional gel electrophoresis and a check for activity preservation by haemagglutination and cell binding (*13*, *26*−*33*). Assessment of carbohydrate-inhibitable binding of the probe to a matrix of neoglycoprotein adsorbed to the surface of plastic microtiter plate wells (0.5 μg/well) was performed in a two-step colorimetric assay, using the presence of 75 mM lactose and 1 mg/mL asialofetuin to interfere with carbohydrate-dependent binding and the streptavidin−peroxidase conjugate (0.5 μg/mL; Sigma) as the indicator conjugate (*13*, *25*). Cell binding of biotinylated neoglycoproteins (25 μg/mL for 8 × 10^6 cells/mL) was routinely assessed in a FACScan instrument (Becton-Dickinson, Heidelberg, Germany) using the fluorescent indicator conjugate streptavidin−R-phycoerythrin (1:40 dilution; Sigma) (*13*, *25*). The complete set of neoglycoproteins was generally processed with cell batches from the same passage at the same time, and prolonged culture periods were avoided to ensure the validity of direct comparison. The panel of tested tumor cells consisted of a B-lymphoblastoid line [Croco II, established in our laboratory (*34*)] and commercially available T-lymphoblastoid (CCRF-CEM), erythroleukemic (K-562), acute myelogenous leukemic (KG-1), mammary (DU4475), and colon carcinoma (C205, SW480, and SW620) lines. To monitor organ distribution in male Ehrlich solid tumor-bearing ddY mice, the neoglycoproteins were radioiodinated by the chloramine-T method using NaI up to a specific radioactivity of 8−10 MBq/mg, and a dose of 80−100 kBq was injected intravenously via the tail vein, after which radioactivity levels in blood and organs were determined and the percentage of injected dose per gram of wet tissue or per milliliter of blood was calculated (*13*).

Computational Procedures. Molecular dynamics (MD) simulations were performed on several Linux personal computers using TINKER (*35*) with the MM3 parametrization (*36*), which was recently shown to be well-suited for studies of carbohydrates (*37*). Different conformations of the unsubstituted complex-type biantennary *N*-glycan and its derivatives harboring either one or both core substitutions

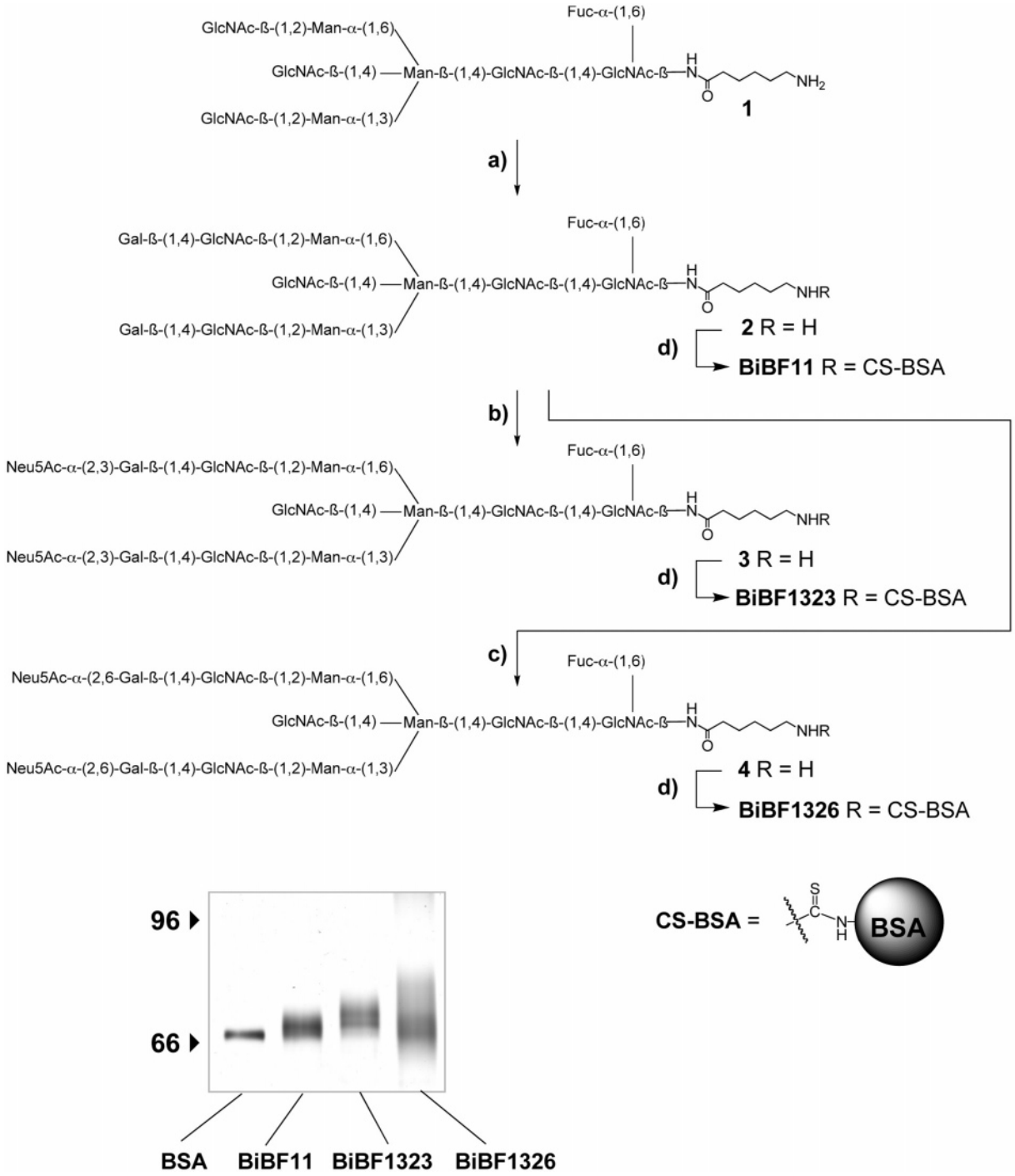

FIGURE 2: Chemical and enzymatic steps to turn the spacered nonasaccharide into fully galactosylated/sialylated *N*-glycans with an isothiocyanate group at the spacer's end for conjugation of the glycan to the carrier protein: (a) UDP-Gal, β1,4-galactosyltransferase, alkaline phosphatase (99%); (b) α2,3-sialyltransferase, CMP-Neu5Ac, alkaline phosphatase (94%); (c) α2,6-sialyltransferase, CMP-Neu5Ac, alkaline phosphatase (47%); and (d) (1) thiophosgene, CH_2Cl_2/H_2O, $NaHCO_3$, (2) BSA, H_2O, $NaHCO_3$. Documentation of results from gel electrophoretic analysis under denaturing and reducing conditions after silver staining (bottom part) is added to illustrate purity and a measure of incorporation yield. Relevant positions of marker proteins at 66 and 96 kDa are indicated by arrowheads, and the lanes for the carbohydrate-free carrier protein BSA and the three neoglycoprotein preparations (BiBF11, BiBF1323, and BiBF1326) are shown from left to right.

were constructed to facilitate thorough conformational sampling during the simulation period (10 ns per simulation) at 300 K. At this temperature, the pyranose ring was not subject to inversions. The aspect of ring conformation was routinely checked by calculation of Cremer-Pople ring puckering parameters (*38*) for each geometry stored in the trajectory file. Pseudoatoms were defined in the arithmetic center of selected rings, and the distances between such pseudoatoms were calculated in describing the conformational flexibility of the glycan chains and the vicinity of sugar moieties. The different geometries of the *N*-glycans obtained from the trajectory files were clustered into conformational families on the basis of their glycosidic torsion angles. The clustering allowed us to discern frequently accessed conformations for each type of *N*-glycan in a strictly equivalent manner, leading from the stepwise clustering/visualization/

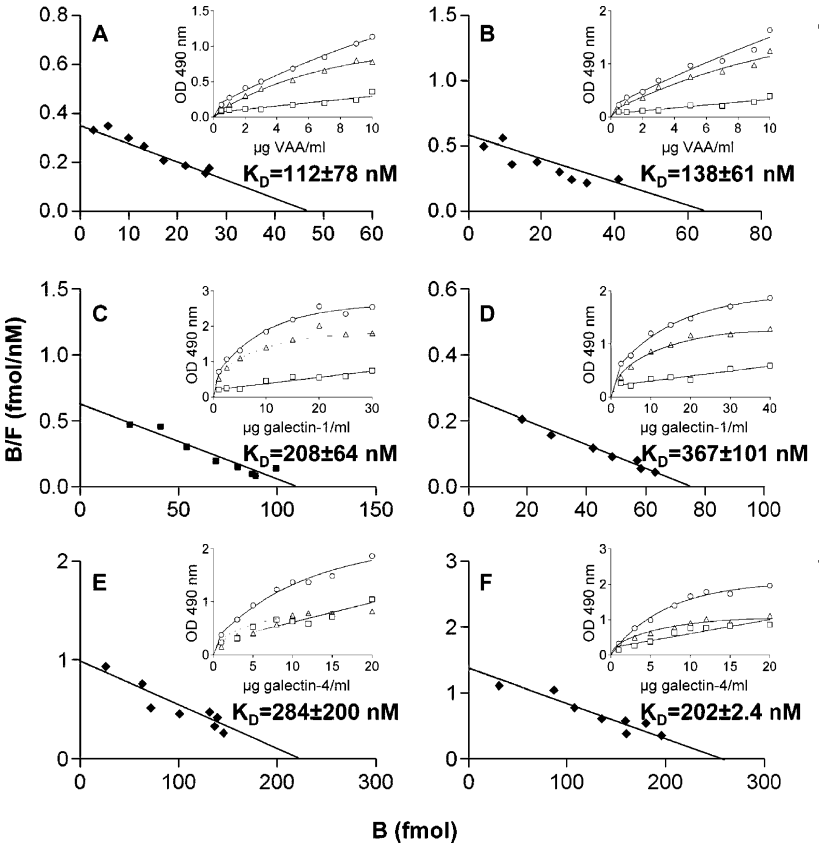

FIGURE 3: Illustration of Scatchard plot analysis of the carbohydrate-inhibitable interaction between the undecasaccharide BiBF11 (left) and the fully α2,3/6-sialylated tridecasaccharides BiBF1323/6 (right) with the mistletoe lectin (A and B), galectin-1 (C and D), and galectin-4 (E and F). The plant lectin also reacted well with the α2,6-sialylated glycan (B), whereas galectins tolerate α2,3-sialylation (D and F). K_D values (mean ± standard deviation) are given for the complete set of analytical data with at least four independent experimental series for each combination of lectin and neoglycoprotein. In the inset, the extent of total binding (○) was reduced by that of the signal which was not suppressed by the presence of glycoinhibitors [(□) 75 mM lactose and 1 mg/mL asialofetuin] to yield the level of carbohydrate-inhibitable binding (△).

comparison approach (self-written programs) to convenient graphical comparison of cluster geometries.

RESULTS

Synthetic and Analytical Chemistry. A chemoenzymatic strategy was followed to convert the spacered nonasaccharide **1** as starting point into fully galactosylated/sialylated *N*-glycans presenting the crucial isothiocyanate group for conjugation to the carrier protein (Figure 2). The individual steps toward the products were routinely monitored by NMR and mass spectrometry. When standard conditions were used, the coupling of the glycans to carbohydrate-free carrier protein was allowed to proceed over a period of 6 days at pH 9, after which glycan incorporation was first demonstrated by a shift in electrophoretic mobility (Figure 2, bottom). Because detergent binding and the staining intensity of the product in gel processing could be influenced by the presence of glycan, especially when sialylated, the number of oligosaccharides per carrier protein was determined by mass spectrometry. Evidence for attachment of up to three *N*-glycans was obtained, and the average conjugation rate was close to 1. With these neoglycoproteins in hand, we could proceed to measure ligand properties of the *N*-glycans in biochemical, in vitro, and in vivo assays under rigorously standardized conditions.

Biochemical Assays. In the first type of assay, ligand properties were assessed after neoglycoproteins were applied to the surface of plastic microtiter plate wells, where they established a matrix with features of a rigid cell surface. Its glycan complexity, however, was confined to a single type of chain. As a counterpart for protein−carbohydrate interaction, a panel of sugar receptors with specificity for β-galactosides and sensitivity to the sialylation status, among them adhesion/growth-regulatory members of the galectin family mentioned in the introduction, was then established. Each protein was purified, labeled, and tested to probe the ligand properties of this matrix. It is important to note that the two core substitutions themselves make no contact with these proteins, as is the case for the plant agglutinins PHA-E and PSA, so that an impact on the mode of branch-end presentation of the galactose residues could be inferred. To examine this aspect thoroughly, binding site orientation and quaternary structure were chosen to differ within this protein panel while the monosaccharide specificity was maintained. In detail, we assayed the toxic mistletoe lectin which is closely related to the biohazard ricin, a member of each galectin subfamily with prototype homodimeric galectin-1, chimera-type galectin-3, and tandem repeat-type galectin-4 as well as the β-galactoside-specific IgG fraction of human serum. Binding of the sugar receptors to the glycan-presenting matrix was invariably saturable and inhibited by cognate sugar (Figure 3). As a further measure of the specificity of the interaction process, the known reactivity toward sialylated glycans was retained. While the plant agglutinin tolerates α2,6-sialylation,

Table 1: Apparent K_D Values (in nanomolar) of the Interaction of Complex-Type Biantennary *N*-Glycans as the Ligand Part of Neoglycoproteins in a Solid-Phase Assay with Different Sugar Receptors[a]

	BiBF11	Bi9	BiF10	BiB10
VAA	112 ± 78	27 ± 12[b]	113 ± 56[c]	163 ± 80[d]
galectin-1	208 ± 64	900 ± 176[b]	377 ± 140[c]	519 ± 118[d]
galectin-3	522 ± 142	388 ± 323	193 ± 52	191 ± 72
galectin-4	284 ± 200	198 ± 44	340 ± 183	226 ± 94
Lac IgG	139 ± 12	33 ± 20[b]	22 ± 1[c]	74 ± 32

[a] For the nomenclature and structures of the *N*-glycans, please see Figure 1. [b] From ref *13*. [c] From ref *24*. [d] From ref *25*.

human galectins can readily accommodate α2,3-sialylated β-galactosides (Figure 3).

Having herewith documented the specificity of the protein−carbohydrate interaction underlying the binding process, we performed systematic interaction studies for each protein. The quantitative data obtained from the Scatchard plots (Figure 3) were then summarized to be set in relation to previously published data sets on the other three types of biantennary *N*-glycans (their structures shown in Figure 1). Inspection of Table 1, presenting this comparative compilation, revealed that the type of *N*-glycan and the properties of the sugar receptor can matter for affinity. Both the plant lectin and galectin-1 provided cases for a clear effect of disubstitution on affinity (BiBF11 vs Bi9). It was not uniform but led to alterations in opposite directions. The disubstitution will apparently weaken toxin binding while favoring galectin-1 association under these conditions. Changes including the decasaccharide BiB10 were apparent for galectin-1 but not for galectin-4, a structural rationalization at present hampered by the current lack of knowledge of the relative orientation of binding sites in this tandem-repeat-type galectin. An impact of quaternary structure was underscored by the case of chimera-type galectin-3. It is predominantly monomeric in solution with a tendency to pentamerize when it contacts multivalent ligands (*39*). Reduction of galectin-3's capacity for oligomer formation by proteolytic removal of the collagenous tail reduced affinity markedly (not shown). As with galectin-3, binding of the IgG fraction was negatively affected by the substitutions (Table 1). These results in a setting with a rigid glycan-bearing surface and a single protein as a probe provided initial support for the concept of affinity regulation by core disubstitution. To further gather evidence for the validity of this hypothesis, we next tested the binding properties of the neoglycoproteins with a panel of human tumor cell lines.

Cell Biological Assays. The labeled markers were incubated with native cells of established lines. Work with this experimental system will supply information about how an *N*-glycan will react with cell surface lectins. To exclude any contribution of the carrier protein to cell binding, we first tested labeled carbohydrate-free albumin and detected no binding under the given conditions even at a high concentration (Figure 4, top row). In contrast, neoglycoproteins bound to cells. Cell positivity depended on the concentration of the markers, and the interaction was inhibited by cognate sugar (Figure 4, bottom row). Glycan conjugation was thus crucial for conveying ligand properties for lectins to the carrier protein. Of note, complex-type biantennary *N*-glycans of the serum pentraxin were more potent as an inhibitor than

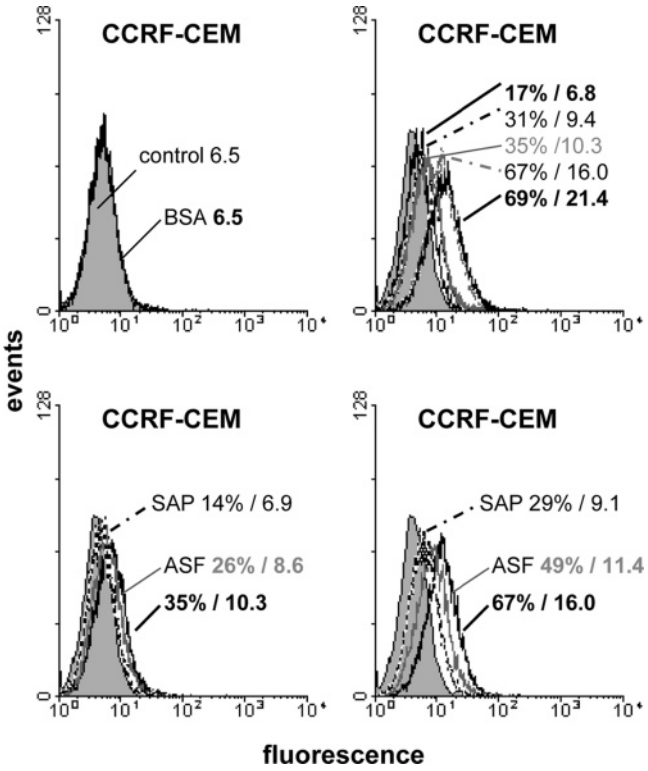

FIGURE 4: Carbohydrate and concentration dependence of cell surface staining using the human T-lymphoblastoid CCRF-CEM line. Quantitative data on a percentage of positive cells (%) and mean channel fluorescence are added to each panel. The gray area depicts the background control. Characteristics of cell surface staining with the carbohydrate-free carrier protein (BSA at a concentration of 25 μg/mL; left) and the neoglycoprotein BiBF11 using different concentrations increasing from 2 μg/mL to 5, 10, 20, and 50 μg/mL (right) are illustrated in the figure's first row. Carbohydrate-dependent inhibition of neoglycoprotein binding was tested using a mixture of 100 mM lactose and 1 mg/mL glycoprotein (human serum amyloid P component, SAP; asialofetuin, ASF) in experiments with 10 (left) or 20 μg/mL (right) labeled neoglycoprotein BiBF11 (second row).

the glycan display of asialofetuin (ASF) with predominantly triantennary chains (Figure 4).

Having substantiated the carbohydrate dependence of binding, we next performed a thorough screening with lines covering common tumor types to add potential clinical relevance. Within the panel of eight lines, significant signals were recorded in four cases, as compiled in Figure 5. The lack of significant binding to cells of four lines already indicated that binding properties of the tested *N*-glycan exhibited characteristic features. The extent to which this staining profile can be singled out from those of the other tested *N*-glycans is shown by comparison in Figure 6. On average, the binding capacity of the neoglycoprotein with the disubstituted *N*-glycan was comparatively low. Individual cases with rather strong reactivity (CCRF-CEM/BiBF11 or SW480/BiBF1326) argued against the incorporation yield being a major factor for a general decrease. Overall, these results defined the relationship between *N*-glycan structure and tumor cell surface staining. When entering circulation, the *N*-glycans will determine the in vivo biodistribution of the neoglycoproteins. Besides the discovery of an impact of the disubstituted *N*-glycans on serum clearance, this characterization has relevance for the quest to set up rules in rational glycoengineering of pharmaproteins or imaging tools.

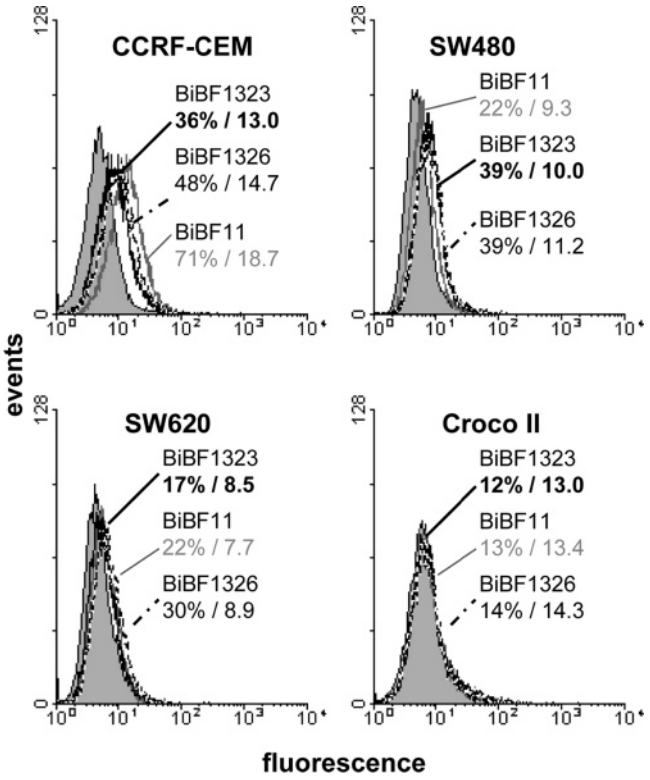

FIGURE 5: Binding of the labeled neoglycoproteins BiBF11, BiBF1323, and BiBF1326 to human tumor cells. Monitoring of tumor cell surface staining is illustrated at the standard concentration of 25 μg/mL for four different lines, i.e., the CCRF-CEM T-lymphoblastoid line, the SW480 and SW620 colon carcinoma lines, and the Croco II B-lymphoblastoid line (for details on quantitative aspects, please see the legend of Figure 4).

They will be essential for reaching optimal pharmacokinetics of a glycoprotein for any clinical purpose.

Monitoring of Biodistribution in Vivo. Instead of biotinylation, samples of the same neoglycoprotein batches were radioiodinated for this purpose. Organ retention and serum clearance were measured after intravenous injection. The obtained results uncovered a strong organ retention and a rather slow clearance rate of the neoglycoprotein with the undecasaccharide BiBF11 as a ligand part (Table 2). Evidently, the core disubstitution hinders branch-end epitopes to match the topology of lectin sites in endocytic asialoglycoprotein receptors. In other words, prolonged serum presence was ensured with this glycan as was retention in liver, kidney, and other organs, and also the solid tumor (Table 2 and Figure 7A,B). As a consequence, this type of natural tailoring of the glycan part of glycoproteins revealed a remarkable capacity to retard clearance despite the presence of terminal galactose units (Figure 7A,B). Therefore, should the prolonged serum presence of a glycoprotein be an aim, the gradual removal of α2,3-linked sialic acids from *N*-glycans, a stop signal for hepatic clearance and here first-line protection, will in this special case not markedly accelerate the elimination of glycoprotein from circulation. This feature renders the α2,3-sialylated disubstituted *N*-glycan (BiBF1323) suited to effectively slow glycoprotein clearance. Because the core substitutions are not contact points for asialoglycoprotein receptors and the number of branch-end galactose units remains constant (please see Figure 1), clues for explaining the measured differences may be tracked down by a computational study. Toward this end, we performed MD simulations.

Computational Chemistry. The aim of this part of the study was to define major aspects of the conformation of the complex-type biantennary *N*-glycan carrying both core substitutions. To identify an assumed effect of the combined presence of both moieties on the core, we monitored the conformational behavior of the unsubstituted nonasaccharide (Bi9) and the two monosubstituted glycans (BiB10 and BiF10) in parallel with identical settings. Complete consideration of the Φ, Ψ, and ω angles adds up to a series of 17 (Bi9), 19 (BiB10), 20 (BiF10), or 22 (BiBF11) parameters. On average, the energy-graded clustering resulted in rather similar conformational parameters for the predominantly adopted structures of *N*-glycans Bi9 and BiF10, whereas BiB10 exhibited altered behavior at the first glycosidic linkage of the α1,3/6-arms (Figure 8). Notably, the presence of both substitutions in the undecasaccharide BiBF11 led to a characteristic pattern with opposite orientations of the α1,6-antenna relative to BiB10 and of the α1,3-antenna relative to Bi9/BiF10 (Figure 8). To support this finding, additional 10 ns simulations at 400 K with different starting geometries, including the Y shape, backfolding in the α1,3-arm, and the extension of the α1,6-arm, were run. In each case, the noted preference was confirmed. In this set of major constellations, the distance between the two galactose units at the branch ends, a key parameter for binding to cell lectins, reaches an average of 5.9 Å for Bi9/BiF10 by backfolding, 8.1 Å for BiB10, and 22.1 Å for BiBF11. Admittedly, flexibility at the crucial α1,3/6-linkages in the trimannoside part of the core will still be operative, resulting in a dynamic equilibrium between extended and backfolded orientations of the α1,3/6-linked branches.

DISCUSSION

The role of glycan epitopes as biochemical signals in intermolecular interactions is already widely appreciated with respect to the lectin-binding groups at branch ends (*11*, *40*). Still, modifications at sites other than the contact points for carbohydrate-specific proteins may factor into binding properties. Indeed, the concept which ascribes the role of molecular switches to the natural non-random core substitutions in *N*-glycans has not only intuitive appeal. Experimental support has come from tracking down the substrate-level control within the biosynthetic pathway toward mature *N*-glycans. For example, the bisecting GlcNAc moiety is a stop signal for *N*-acetylglucosaminyltransferases II, IV, and V and for the α1,6-fucosyltransferase (*3*). Moreover, cell models engineered for an increased level of expression of a distinct glycosyltransferase are allowing delineation of specific functions of distinct glycans on the level of a certain protein. Core fucosylation as an apparently intramolecular modulator for growth factor activities on the level of receptor characteristics has already been mentioned in the introductory section (*7*). Moreover, cell functions such as the integrin-mediated invasivity of glioma or migration of neuroblastoma cells are affected when the frequency of β1,6-branching versus bisecting GlcNAc is altered (*41*, *42*). Even more intriguing, the practice of being able to select CHO glycosylation mutants due to their acquisition of resistance to toxic plant lectins (*43*) signals that changes in the glycomic cell surface profile can protect the cells from harmful protein−

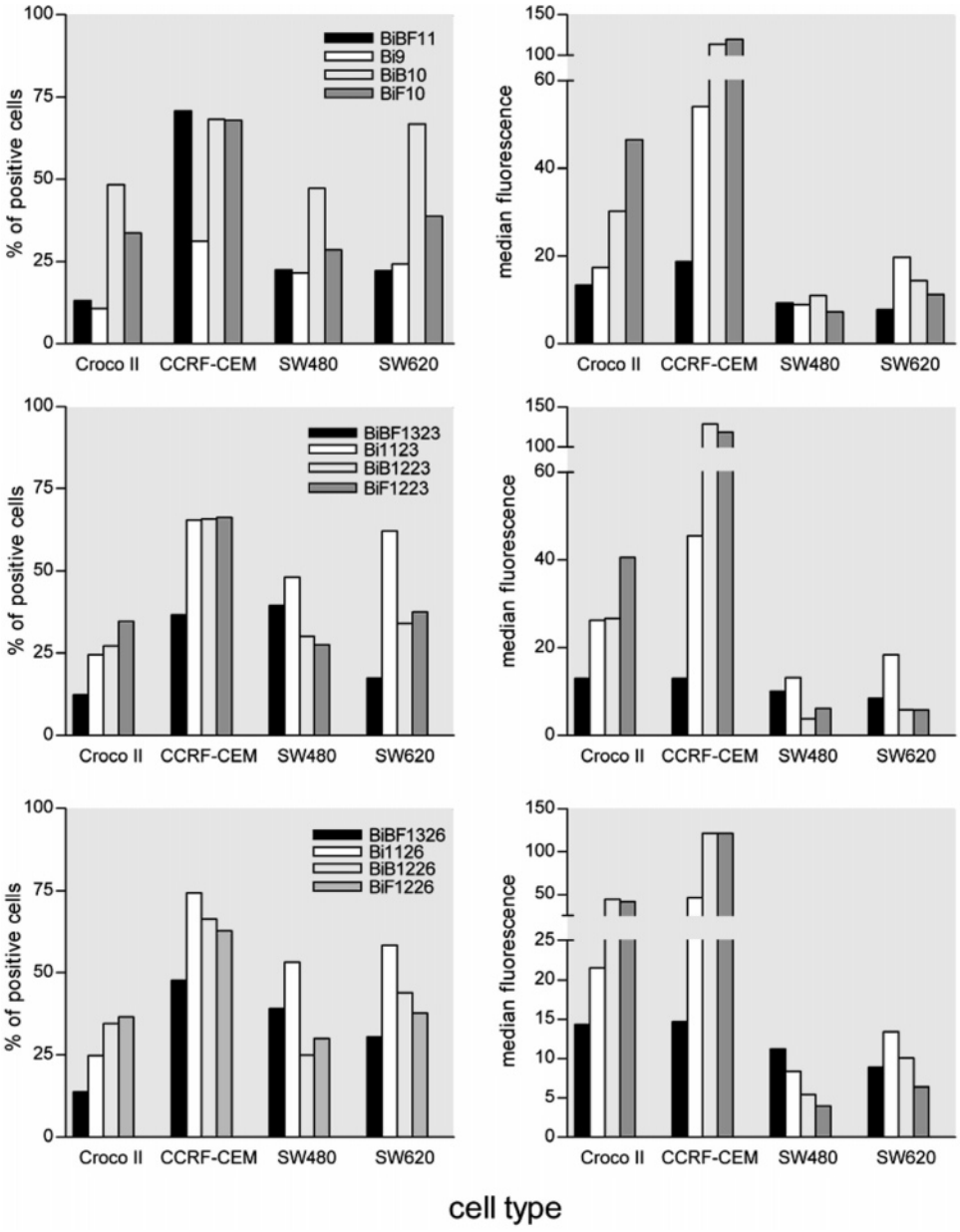

FIGURE 6: Comparison of fluorescent cell surface staining (left panel, percent of positive cells; right panel, median fluorescence) by each of the three neoglycoproteins carrying the undecasaccharide (BiBF11, first row) or the α2,3/α2,6-sialylated tridecasaccharides (BiBF1323, second row; BiBF1326, third row) with cell reactivity for un- or monosubstituted *N*-glycans. Results from previous reports on the corresponding *N*-glycans without core substitution (Bi9, Bi1123, and Bi1126) and with either the bisecting GlcNAc moiety (BiB10, BiB1223, and BiB1226) or the core-fucose unit (BiF10, BiF1223, and BiF1226) (*13*, *24*, *25*) are given in each panel. Standard deviations within experimental series were generally less than 7.5%.

carbohydrate interactions. That said, it is of course tempting to view the known set of glycan substitutions, especially the core modifications, as natural regulators of affinity also to endogenous lectins, giving shifts in the glycomic profile a functional dimension in biorecognition in situ.

This study details respective consequences of the simultaneous presence of core-fucose and bisecting GlcNAc entities in complex-type biantennary *N*-glycans. For this purpose, we have devised a combined strategy using synthetic chemistry and three types of bioassays. To experimentally test the biorecognitive capacity of the core-disubstituted *N*-glycan, we prepared neoglycoproteins with a spacered oligosaccharide as the ligand part. Because the extent of natural production of core-fucosylated biantennary *N*-glycans with complete sialylation can be rather low (*44*), our approach has the added advantage of gaining access to the α2,3/6-sialylated compounds. Their conjugation to a cytochemically inert carrier led to the neoglycoproteins, the spacer avoiding intimate contacts with the protein surface in the core region. Although protein site-specific glycosylation can be an issue for affinity regulation (*11*), it was our aim here to focus exclusively on glycan properties. The yield of the chemical attachment of *N*-glycan to the protein was comparatively low for the core-disubstituted *N*-glycans on the basis of previous experience with un- or monosubstituted compounds under identical conditions yielding average incorporation of 2.4−4.9 *N*-glycan per carrier (*13*, *24*, *25*). Of note, these results corresponded well with the extent of incorporation of triantennary *N*-glycans with an average of 1−1.5 *N*-glycans per BSA molecule (*45*). Except for this

Table 2: Biodistribution of Neoglycoproteins with Complex-Type Biantennary Un- and Tridecasaccharides Containing Core Fucosylation and Bisecting GlcNAc Residues as the Ligand Part in Ehrlich Solid Tumor-Bearing Mice (% injected dose per gram of tissue or milliliter of blood) after 1 and 6 h[a]

	1 h			6 h		
tissue type	BiBF11	BiBF1323	BiBF1326	BiBF11	BiBF1323	BiBF1326
blood	26.32 ± 4.35	31.80 ± 4.20	17.23 ± 6.55	4.15 ± 1.41	16.88 ± 4.78	9.22 ± 2.96
liver	8.63 ± 1.15	6.54 ± 1.88	25.81 ± 9.75	3.67 ± 0.57	3.76 ± 0.59	4.51 ± 0.80
kidneys	8.22 ± 0.75	8.59 ± 1.03	11.71 ± 1.03	2.88 ± 0.47	4.59 ± 0.99	4.70 ± 0.38
spleen	4.34 ± 0.33	4.46 ± 1.28	7.41 ± 1.06	1.74 ± 0.31	2.52 ± 0.40	2.82 ± 0.44
heart	5.00 ± 0.26	5.15 ± 0.79	4.02 ± 1.25	1.19 ± 0.39	3.37 ± 1.12	2.18 ± 0.66
lungs	5.07 ± 0.46	4.64 ± 0.91	5.76 ± 1.32	1.82 ± 0.47	4.17 ± 1.01	2.64 ± 0.51
thymus	1.69 ± 0.40	2.05 ± 0.82	3.19 ± 0.53	1.02 ± 0.27	1.98 ± 0.65	1.52 ± 0.32
pancreas	3.17 ± 0.48	2.66 ± 0.59	4.64 ± 0.57	1.36 ± 0.31	2.29 ± 0.46	1.88 ± 0.54
muscle	1.61 ± 0.25	1.72 ± 0.56	1.62 ± 0.34	0.58 ± 0.13	1.04 ± 0.41	0.80 ± 0.19
brain	0.54 ± 0.05	0.59 ± 0.07	0.48 ± 0.10	0.12 ± 0.03	0.30 ± 0.07	0.19 ± 0.04
tumor	5.57 ± 0.57	5.45 ± 0.98	5.58 ± 1.55	2.79 ± 0.88	6.04 ± 1.60	4.15 ± 0.78
lymph node	4.90 ± 0.69	3.93 ± 2.36	5.36 ± 1.85	1.32 ± 0.20	3.58 ± 1.28	3.27 ± 1.19

[a] Each value indicates the mean ± standard deviation for four to five mice.

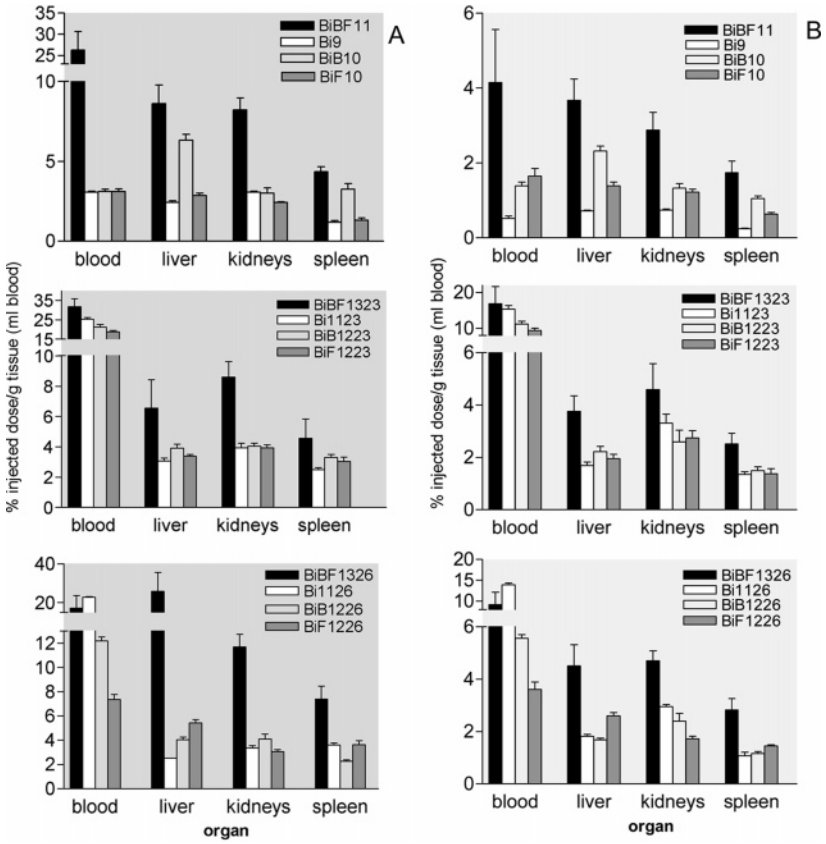

FIGURE 7: Comparison of glycan-type-dependent biodistribution profiles of radioiodinated neoglycoproteins 1 (A) and 6 h (B) after their intravenous injection into tumor-bearing mice. The results presented in Table 2 are set in relation to previously published data (*13*, *24*, *25*) for the *N*-glycans without core substitution (Bi9, Bi1123, and Bi1126) and the derivatives containing either the bisecting GlcNAc moiety (BiB10, BiB1223, and BiB1226) or the core-fucose unit (BiF10, BiF1223, and BiF1226). Data sets for the four types of sialic acid-free *N*-glycans are presented in the top row, for fully α2,3-sialylated *N*-glycans in the middle row, and for fully α2,6-sialylated *N*-glycans in the bottom row.

factor, all experimental conditions were deliberately kept constant to facilitate comparison between the data sets on *N*-glycans as ligands in the bioassays.

That protein−carbohydrate interactions are responsible for the measured binding was unequivocally ascertained by inhibition using cognate sugars. Ligand recognition by dimeric lectins in the solid-phase assay will most likely engage different *N*-glycan chains, as observed previously in precipitation analysis in solution (*46*). Although separated by only 15 Å, the two sites for galactose accommodation in the plant agglutinin characterized by a central Trp residue are only partially accessible so that the two domains with central Tyr moieties which are 87 Å apart will be operative (*32*, *47*). In human galectin-1, the two contact sites are separated by 44 Å (*48*). The presented evidence for a type-dependent relationship among the sugar receptors with respect to affinity is in accord with non-identical functional profiles of galectins (*11*, *12*). Tailoring of the glycan's end group and, as described herein, its topological presentation can thus have a bearing on affinity. In this sense, effects of natural epitope clustering on binding, also measured with a solid-phase assay, are in line with the given results (*49*−

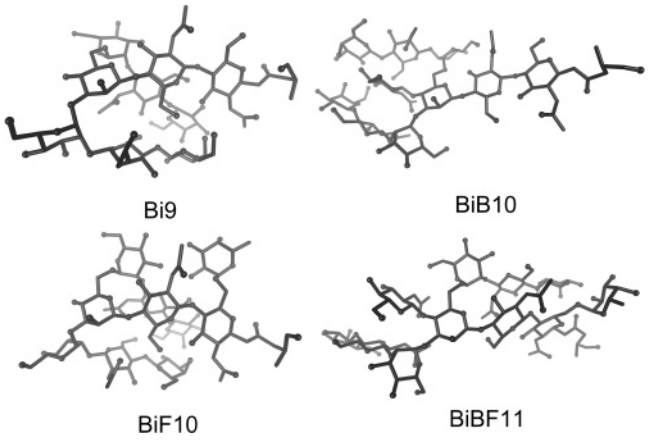

FIGURE 8: Illustration of representative conformations from each of the most densely populated clusters in the cases of the complex-type biantennary *N*-glycans Bi9, BiB10, BiF10, and BiBF11 (for schemes of structures, please see Figure 1). Backfolding of the α1,3-arm (Bi9 and BiF10) and the α1,6-arm (Bi9, BiF10, and BiBF11) is apparent.

51). Should it be justified to reliably liken the matrix in the solid-phase assay to a rigid cell surface with one type of ligand, the order of the data will then be similar to that determined in assays on cell surfaces with one predominant ligand type. The human SK-N-MC neuroblastoma model and galectin preference for the pentasaccharide of ganglioside GM_1 on the cell surface provide an opportunity to carry out this comparison, and the determination of K_D values in the range of several hundred nanomolar with native cell surfaces as the reactive site supports the drawn analogy (*52*, *53*). Moreover, in line with the decreased affinity for galectin-3 in the solid-phase assay, this lectin's reactivity with LEC10 CHO mutant cells which produce core-disubstituted *N*-glycans was reduced (*54*). The same holds true when increased resistance against toxicity of ricin (*20*) is related to the decreased affinity for the related AB-toxin VAA. However, the activation of expression of *N*-acetylglucosaminyltransferase III in this mutant can also bring about changes in the branching profile that will confound the interpretation (*20*−*22*, *54*). At any rate, the solid-phase assay proved to be diagnostic for delineating K_D differences dependent on core substitution. They can reach the order of 4−6-fold changes. This assay's capacity to sense the impact of structural changes in the ligand on lectin reactivity has also been documented in another, less frequent case of core substitution. When the GlcNAc moiety was shifted from the bisecting β1,4- to the β1,2-position to yield the LEC14 epitope and then galactosylated, a slight decrease in galectin-1 reactivity ensued (*55*).

The following biological assays move the results further into the realm of potential applications. It is noteworthy that the core-disubstituted *N*-glycan on average has a reduced capacity for cell binding, another strong indicator of a structure−(ligand) activity relation in this case. Assumedly, core disubstitution may therefore preferentially be relevant for establishing intramolecular contacts in situ, a prominent case being IgG glycosylation. That intermolecular ligand properties are apparently reduced was underscored by analysis of the biodistribution. In this respect, the characteristic effects on serum clearance and organ retention are even likely to offer a promising perspective for rational glycoengineering. First, the presented results extended the evidence for specific clearance routes of α2,6-sialylated glycans, with an opposing effect of α2,3-sialylation introduced by the sialyltransferase ST3Gal-IV (*56*−*58*). Second and even more importantly, the strict topological requirement for homing on to the subunits of the hepatic asialoglycoprotein receptor is evidently not fulfilled well by the core-disubstituted *N*-glycan, although it presents two galactose units at the branch ends. If reflecting an insufficient match between these contact points and the highly ordered pattern of complementary sites in the liver lectins, characteristic conformational preferences should underlie the differential clearance characteristics. This is why we used MD simulations to comparatively describe major conformational consequences of core substitution.

Indeed, core substitutions can make their presence felt by long-range effects on the relative positioning of branch-end residues (Figure 8). In other words, the shape equilibrium adopted by an oligosaccharide can be affected. A characteristic constellation of the disubstituted undecasaccharide BiBF11 was delineated in silico relative to the unsubstituted nonasaccharide Bi9 and the two monosubstituted *N*-glycans BiB10 and BiF10. Evidently, the conformational space accessed by the branch-end moieties, which are common contact points for tissue lectins (*11*), is differentially structured by the core substitutions. This impact offers a possibility of rationalizing the bioassay data in structural terms. In summary, the presented results clearly epitomize a role of core disubstitution in the regulation of glycan biorecognition. Having detected these substitution-dependent differences and a role of the natural core substitutions as molecular switches, we are now able to further exploit the given strategy for the design of new variants with unnatural core substitutions in fully realizing the emerging potential of glycoengineering in vivo.

ACKNOWLEDGMENT

We gratefully acknowledge Dr. H. Crampus, Dr. B. Friday, Dr. E. Miyoshi, and Dr. S. Namirha for inspiring discussions and B. Hofer and L. Mantel for excellent technical assistance.

REFERENCES

1. Sharon, N., and Lis, H. (1997) Glycoproteins: Structure and Function, in *Glycosciences: Status and Perspectives* (Gabius, H.-J., and Gabius, S., Eds.) pp 133−162, Chapman & Hall, Weinheim. Germany.
2. Reuter, G., and Gabius, H.-J. (1999) Eukaryotic glycosylation: Whim of nature or multipurpose tool? *Cell. Mol. Life Sci. 55*, 368−422.
3. Brockhausen, I., and Schachter, H. (1997) Glycosyltransferases Involved in N- and O-Glycan Biosynthesis, in *Glycosciences: Status and Perspectives* (Gabius, H.-J., and Gabius, S., Eds.) pp 79−113, Chapman & Hall, Weinheim, Germany.
4. Gabius, H.-J., Siebert, H.-C., André, S., Jiménez-Barbero, J., and Rüdiger, H. (2004) Chemical biology of the sugar code, *ChemBioChem 5*, 740−764.
5. Lowe, J. B., and Marth, J. D. (2003) A genetic approach to mammalian glycan function, *Annu. Rev. Biochem. 72*, 643−691.
6. Suzuki, T., Kitajima, K., Inoue, S., and Inoue, Y. (1997) Occurrence and Potential Functions of N-Glycanases, in *Glycosciences: Status and Perspectives* (Gabius, H.-J., and Gabius, S., Eds.) pp 121−131, Chapman & Hall, Weinheim, Germany.
7. Wang, X., Gu, J., Ihara, H., Miyoshi, E., Honke, K., and Taniguchi, N. (2006) Core fucosylation regulates epidermal growth factor receptor-mediated intracellular signaling, *J. Biol. Chem. 281*, 2572−2577.

8. Gabius, H.-J. (1997) Animal lectins, *Eur. J. Biochem. 243*, 543−576.
9. Partridge, E. A., Le Roy, C., Di Guglielmo, G. M., Pawling, J., Cheung, P., Granovsky, M., Nabi, I. R., Wrana, J. L., and Dennis, J. W. (2004) Regulation of cytokine receptors by Golgi N-glycan processing and endocytosis, *Science 306*, 120−124.
10. Ohtsubo, K., Takamatsu, S., Minowa, M. T., Yoshida, A., Takeuchi, M., and Marth, J. D. (2005) Dietary and genetic control of glucose transporter 2 glycosylation promotes insulin secretion in suppressing diabetes, *Cell 123*, 1307−1321.
11. Gabius, H.-J. (2006) Cell surface glycans: The why and how of their functionality as biochemical signals in lectin-mediated information transfer, *Crit. Rev. Immunol. 26*, 43−79.
12. Villalobo, A., Nogales-González, A., and Gabius, H.-J. (2006) A guide to signaling pathways connecting protein-glycan interaction with the emerging versatile effector functionality of mammalian lectins, *Trends Glycosci. Glycotechnol. 18*, 1−37.
13. André, S., Unverzagt, C., Kojima, S., Dong, X., Fink, C., Kayser, K., and Gabius, H.-J. (1997) Neoglycoproteins with the synthetic complex biantennary nonasaccharide or its α2,3/α2,6-sialylated derivatives: Their preparation, assessment of their ligand properties for purified lectins, for tumor cells *in vitro*, and in tissue sections, and their biodistribution in tumor-bearing mice, *Bioconjugate Chem. 8*, 845−855.
14. Ohno, M., Nishikawa, A., Koketsu, M., Taga, H., Endo, Y., Hada, T., Higashino, K., and Taniguchi, N. (1992) Enzymatic basis of sugar structures of α-fetoprotein in hepatoma and hepatoblastoma cell lines: Correlation with activities of α1-6 fucosyltransferase and N-acetylglucosaminyltransferases III and V, *Int. J. Cancer 51*, 315−317.
15. Grey, A. A., Narasimhan, S., Brisson, J. R., Schachter, H., and Carver, J. P. (1982) Structures of the glycopeptides of a human γ1-immunoglobulin G (Tem) myeloma protein as determined by 360-megahertz nuclear magnetic resonance spectroscopy, *Can. J. Chem. 60*, 1123−1131.
16. Raju, T. S., Briggs, J. B., Borge, S. M., and Jones, A. J. S. (2000) Species-specific variation in glycosylation of IgG: Evidence for the species-specific sialylation and branch-specific galactosylation and importance for engineering recombinant glycoprotein therapeutics, *Glycobiology 10*, 477−486.
17. Shinkawa, T., Nakamura, K., Yamane, N., Shoji-Hosaka, E., Kanda, Y., Sakurada, M., Uchida, K., Anazawa, H., Satoh, M., Yamasaki, M., Hanai, N., and Shitara, K. (2003) The absence of fucose but not the presence of galactose or bisecting N-acetylglucosamine of human IgG_1 complex-type oligosaccharides shows the critical role of enhancing antibody-dependent cellular cytotoxicity, *J. Biol. Chem. 278*, 3466−3473.
18. Okazaki, A., Shoji-Hosaka, E., Nakamura, K., Wakitani, M., Uchida, K., Kakita, S., Tsumoto, K., Kumagai, I., and Shitara, K. (2004) Fucose depletion from human IgG_1 oligosaccharide enhances binding enthalpy and association rate between IgG_1 and FcγRIIIa, *J. Mol. Biol. 336*, 1239−1249.
19. Ferrara, C., Stuart, F., Sondermann, P., Brünker, P., and Umaña, P. (2006) The carbohydrate at FcγRIIIa Asn-162. An element required for high affinity binding to non-fucosylated IgG glycoforms, *J. Biol. Chem. 281*, 5032−5036.
20. Campbell, C., and Stanley, P. (1984) A dominant mutation to ricin resistance in Chinese hamster ovary cells induces UDP-GlcNAc: glycopeptide β-4-N-acetylglucosaminyltransferase III activity, *J. Biol. Chem. 256*, 13370−13378.
21. Stanley, P., Sundaram, S., and Sallustio, S. (1991) A subclass of cell surface carbohydrates revealed by a CHO mutant with two glycosylation mutations, *Glycobiology 1*, 307−314.
22. Stanley, P., Sundaram, S., Tang, J., and Shi, S. (2005) Molecular analysis of three gain-of-function CHO mutants that add the bisecting GlcNAc to N-glycans, *Glycobiology 15*, 43−53.
23. Schuberth, R., and Unverzagt, C. (2005) Synthesis of a N-glycan nonasaccharide of the bisecting type with additional core-fucose, *Tetrahedron Lett. 46*, 4201−4204.
24. Unverzagt, C., André, S., Seifert, J., Kojima, S., Fink, C., Srikrishna, G., Freeze, H., Kayser, K., and Gabius, H.-J. (2002) Structure-activity profiles of complex biantennary glycans with core fucosylation and with/without additional α2,3/α2,6 sialylation: Synthesis of neoglycoproteins and their properties in lectin assays, cell binding, and organ uptake, *J. Med. Chem. 45*, 478−491.
25. André, S., Unverzagt, C., Kojima, S., Frank, M., Seifert, J., Fink, C., Kayser, K., von der Lieth, C.-W., and Gabius, H.-J. (2004) Determination of modulation of ligand properties of synthetic complex-type biantennary N-glycans by introduction of bisecting GlcNAc *in silico*, *in vitro* and *in vivo*, *Eur. J. Biochem. 271*, 118−134.
26. Gabius, H.-J. (1990) Influence of type of linkage and spacer on the interaction of β-galactoside-binding proteins with immobilized affinity ligands, *Anal. Biochem. 189*, 91−94.
27. Kopitz, J., von Reitzenstein, C., André, S., Kaltner, H., Uhl, J., Ehemann, V., Cantz, M., and Gabius, H.-J. (2001) Negative regulation of neuroblastoma cell growth by carbohydrate-dependent surface binding of galectin-1 and functional divergence from galectin-3, *J. Biol. Chem. 276*, 35917−35923.
28. Kopitz, J., André, S., von Reitzenstein, C., Versluis, K., Kaltner, H., Pieters, R. J., Wasano, K., Kuwabara, I., Liu, F.-T., Cantz, M., Heck, A. J. R., and Gabius, H.-J. (2003) Homodimeric galectin-7 (p53-induced gene 1) is a negative growth regulator for human neuroblastoma cells, *Oncogene 22*, 6277−6288.
29. Purkrábková, T., Smetana, K., Jr., Dvořánková, B., Holíková, Z., Böck, C., Lensch, M., André, S., Pytlík, R., Liu, F.-T., Klíma, J., Smetana, K., Motlík, J., and Gabius, H.-J. (2003) New aspects of galectin functionality in nuclei of cultured bone marrow stromal and epidermal cells: Biotinylated galectins as tool to detect specific binding sites, *Biol. Cell 95*, 535−545.
30. André, S., Kaltner, H., Furuike, T., Nishimura, S.-I., and Gabius, H.-J. (2004) Persubstituted cyclodextrin-based glycoclusters as inhibitors of protein-carbohydrate recognition using purified plant and mammalian lectins and wild-type and lectin-gene-transfected tumor cells as targets, *Bioconjugate Chem. 15*, 87−98.
31. Dam, T. K., Gabius, H.-J., André, S., Kaltner, H., Lensch, M., and Brewer, C. F. (2005) Galectins bind to the multivalent glycoprotein asialofetuin with enhanced affinities and a gradient of decreasing binding constants, *Biochemistry 44*, 12564−12571.
32. Jiménez, M., Saíz, J. L., André, S., Gabius, H.-J., and Solís, D. (2005) Monomer/dimer equilibrium of the AB-type lectin from mistletoe enables combination of toxin/agglutinin activities in one protein: Analysis of native and citraconylated proteins by ultracentrifugation/gel filtration and cell biological consequences of dimer destabilization, *Glycobiology 15*, 1386−1395.
33. André, S., Pei, Z., Siebert, H.-C., Ramström, O., and Gabius, H.-J. (2006) Glycosyldisulfides from dynamic combinatorial libraries as O-glycoside mimetics for plant and endogenous lectins: Their reactivities in solid-phase and cell assays and conformational analysis by molecular dynamics simulations, *Bioorg. Med. Chem. 14*, 6314−6326.
34. Gabius, S., Joshi, S. S., Gabius, H.-J., and Sharp, J. G. (1991) Establishment, characterization and determination of cell surface sugar receptor (lectin) expression by neoglycoenzymes of a human myeloid marker-expressing B lymphoblastoid cell line, *Anticancer Res. 11*, 793−800.
35. Ponder, J. W. (2004) *User's Guide for THINKER Version 4.2*, Washington University School of Medicine, St. Louis.
36. Allinger, N. L., Yuh, Y. H., and Lii, J.-H. (1989) Molecular mechanics. The MM3 force field for hydrocarbons, *J. Am. Chem. Soc. 111*, 8551−8566.
37. Stortz, C. A. (2005) Comparative performances of MM3(92) and two TINKER MM3 versions for the modeling of carbohydrates, *J. Comput. Chem. 26*, 471−483.
38. Cremer, D., and Pople, J. A. (1975) A general definition of ring puckering coordinates, *J. Am. Chem. Soc. 97*, 1354−1358.
39. Ahmad, N., Gabius, H.-J., André, S., Kaltner, H., Sabesan, S., Roy, R., Liu, B., Macaluso, F., and Brewer, C. F. (2004) Galectin-3 precipitates as a pentamer with synthetic multivalent carbohydrates and forms heterogeneous cross-linked complexes, *J. Biol. Chem. 279*, 10841−10847.
40. Gabius, H.-J., André, S., Kaltner, H., and Siebert, H.-C. (2002) The sugar code: Functional lectinomics, *Biochim. Biophys. Acta 1572*, 165−177.
41. Yamamoto, H., Swoger, J., Greene, S., Saito, T., Hurh, J., Sweeley, C., Leestma, J., Mkrdichian, E., Cerullo, L., Nishikawa, A., Ihara, Y., Taniguchi, N., and Moskal, J. R. (2000) β1,6-N-Acetylglucosamine-bearing N-glycans in human gliomas: Implications for a role in regulating invasivity, *Cancer Res. 60*, 134−142.
42. Zhao, Y., Nakagawa, T., Itoh, S., Inamori, K.-i., Isaji, T., Kariya, Y., Kondo, A., Miyoshi, E., Miyazaki, K., Kawasaki, N., Taniguchi, N., and Gu, J. (2006) N-Acetylglucosaminyltransferase III antagonizes the effect of N-acetylglucosaminyltransferase V on $\alpha_3\beta_1$ integrin-mediated cell migration, *J. Biol. Chem. 281*, 32122−32130.
43. Stanley, P. (1983) Selection of lectin-resistant mutants of animal cells, *Methods Enzymol. 96*, 157−184.

44. Sturla, L., Fruscione, F., Noda, K., Miyoshi, E., Taniguchi, N., Contini, P., and Tonetti, M. (2005) Core fucosylation of N-linked glycans in leukocyte adhesion deficiency/congenital disorder of glycosylation IIc fibroblasts, *Glycobiology 15*, 924−934.
45. André, S., Kojima, S., Gundel, G., Russwurm, R., Schratt, X., Unverzagt, C., and Gabius, H.-J. (2006) Branching mode in complex-type triantennary N-glycans as regulatory element of their ligand properties, *Biochim. Biophys. Acta 1760*, 768−782.
46. Gupta, D., Kaltner, H., Dong, X., Gabius, H.-J., and Brewer, C. F. (1996) Comparative cross-linking activities of lactose-specific plant and animal lectins and a natural lactose-binding immunoglobulin G fraction from human serum with asialofetuin, *Glycobiology 6*, 843−849.
47. Jimenez, M., André, S., Siebert, H.-C., Gabius, H.-J., and Solís, D. (2006) AB-type lectin (toxin/agglutinin) from mistletoe: Differences in affinity of the two galactoside-binding Trp/Tyr-sites and regulation of their functionality by monomer/dimer equilibrium, *Glycobiology 16*, 926−937.
48. López-Lucendo, M. F., Solís, D., André, S., Hirabayashi, J., Kasai, K.-i., Kaltner, H., Gabius, H.-J., and Romero, A. (2004) Growth-regulatory human galectin-1: Crystallographic characterisation of the structural changes induced by single-site mutations and their impact on the thermodynamics of ligand binding, *J. Mol. Biol. 343*, 957−970.
49. Wu, A. M., Wu, J. H., Liu, J.-H., Singh, T., André, S., Kaltner, H., and Gabius, H.-J. (2004) Effects of polyvalency of glycotopes and natural modifications of human blood group ABH/Lewis sugars at the Galβ1-terminated core saccharides on the binding of domain-I of recombinant tandem-repeat-type galectin-4 from rat gastrointestinal tract (G4-N), *Biochimie 86*, 317−326.
50. Wu, A. M., Singh, T., Wu, J. H., Lensch, M., André, S., and Gabius, H.-J. (2006) Interaction profile of galectin-5 with free saccharides and mammalian glycoproteins: Probing its fine specificity and the effect of naturally clustered ligand presentation, *Glycobiology 16*, 524−537.
51. Wu, A. M., Singh, T., Liu, J.-H., Krzeminski, M., Russwurm, R., Siebert, H.-C., Bonvin, A. M. J. J., André, S., and Gabius, H.-J. (2007) Activity-structure correlations in divergent lectin evolution: Fine specificity of chicken galectin CG-14 and computational analysis of flexible ligand docking for CG-14 and the closely related CG-16, *Glycobiology 17*, 165−184.
52. Kopitz, J., von Reitzenstein, C., Burchert, M., Cantz, M., and Gabius, H.-J. (1998) Galectin-1 is a major receptor for ganglioside GM_1, a product of the growth-controlling activity of a cell surface ganglioside sialidase, on human neuroblastoma cells in culture, *J. Biol. Chem. 273*, 11205−11211.
53. André, S., Kaltner, H., Lensch, M., Russwurm, R., Siebert, H.-C., Fallsehr, C., Tajkhorshid, E., Heck, A. J. R., von Knebel Doeberitz, M., Gabius, H.-J., and Kopitz, J. (2005) Determination of structural and functional overlap/divergence of five proto-type galectins by analysis of the growth-regulatory interaction with ganglioside GM_1 *in silico* and *in vitro* on human neuroblastoma cells, *Int. J. Cancer 114*, 46−57.
54. Patnaik, S. K., Potvin, B., Carlsson, S., Sturm, D., Leffler, H., and Stanley, P. (2006) Complex N-glycans are the major ligands for galectins-1, -3, and -8 on Chinese hamster ovary cells, *Glycobiology 16*, 305−317.
55. André, S., Kojima, S., Prahl, I., Lensch, M., Unverzagt, C., and Gabius, H.-J. (2005) Introduction of extended LEC14-type branching into core-fucosylated biantennary N-glycan, *FEBS J. 272*, 1986−1998.
56. Ellies, L. G., Ditto, D., Levy, G. G., Wahrenbrock, M., Ginsburg, D., Varki, A., Le, D. T., and Marth, J. D. (2002) Sialyltransferase ST3Gal-IV operates as a dominant modifier of hemostasis by concealing asialoglycoprotein receptor ligands, *Proc. Natl. Acad. Sci. U.S.A. 99*, 10042−10047.
57. Park, E. I., and Baenziger, J. U. (2004) Closely related mammals have distinct asialoglycoprotein receptor carbohydrate specificities, *J. Biol. Chem. 279*, 40954−40959.
58. Park, E. I., Mi, Y., Unverzagt, C., Gabius, H.-J., and Baenziger, J. U. (2005) The asialoglycoprotein receptor clears glycoconjugates terminating with sialic acid α2,6GalNAc, *Proc. Natl. Acad. Sci. U.S.A. 102*, 17125−17129.

BI7000467